URSI GASS 2020, Rome, Italy, 29 August - 5 September 2020

Design and Development of a Wide-Field Fully Cryogenic Phased Array Feed for Arecibo

Mitchell C. Burnett*(1), Jakob Kunzler(1), Erich Nygaard(1), Brian D. Jeffs(1), Karl F. Warnick(1), Donald Campbell(2), German Cortes-Medellin(2), Stephen Parshley(2), Amit Vishwas(2), Phil Perillat(3) and D. Anish Roshi(3)
(1) Brigham Young University, Provo, UT 84602, USA
(2) Cornell University, Ithaca, NY 14853, USA
(3) Arecibo Observatory, Arecibo, Puerto Rico 00612, USA

Abstract

Brigham Young University (BYU), in collaboration with Cornell University, is developing the Advanced Cryogenic L-band Phased Array Camera for Arecibo (ALPACA) as a user provided facility instrument on the Arecibo 305 m radio telescope. This instrument will consist of a fully cryogenic 69-element phased array feed (PAF) and real-time digital beamformer back end capable of producing 40 simultaneous dual polarized beams with approximately 305 MHz of instantaneous bandwidth at 1.4 GHz. The target design goal is to operate with a system noise temperature of 25 K. We report on simulation results and a preliminary overview of the design and progress of the instrument's development.

1 Introduction

Radio telescopes are important tools for the study of the temporal, spatial, spectral and polarization properties of celestial objects. At decimeter wavelengths and above, a limiting factor for large reflector antennas is the small field of view (FoV). Multi-horn or cluster feed array systems such as the ALFA receiver on the Arecibo Telescope have demonstrated an advantage by increasing the FoV. These multi-horn systems have the disadvantage that the beams are separated by more than the half-power beam width on the sky and mechanically steering the telescope is required to image a contiguous field.

To further expand the instantaneous FoV of the Arecibo radio telescope we are developing a PAF, the Advanced Cryogenic L-band Phased Array Camera for Arecibo (ALPACA). This instrument will have 69 cryogenic dual polarized dipole elements, with RF-over-fiber (RFoF) signal transport, and a real-time beamforming digital back end producing 40 simultaneous dual polarized beams. The digital back end combines the Xilinx RF System on Chip (RFSoC) for direct sampling at L-band with an array of GPU processing nodes for array calibration and various observation modes, including coarse and fine beamformed spectrometers. This paper highlights a few of the challenging requirements for the ALPACA instrument and how we have addressed them in our design.

2 Front End

2.1 Antenna Feed Geometry Modeling

Proper placement and electromagnetic design of the dipole antennas within the PAF are both crucial to maximizing performance of the instrument. This is because effective beam area and system noise characteristics are dependent on the physical design and location of the antennas relative to each other and with respect to the reflector optics. This dependence and its effects on the sensitivity of the instrument over the FoV is combined into one figure of merit known as the survey speed. This is a measure of the relative amount of time required to complete a survey, and is computed as

$$\mathrm{S} = \int_{\mathrm{FOV}} \frac{A_e^2(\Omega)}{T_{\mathrm{sys}}^2(\Omega)} B \, d\Omega \tag{1}$$

where S is survey speed, A_e is the effective aperture, T_{sys} is the system noise temperature, B the bandwidth, and the integral is computed over all steered beam angles Ω in the FoV [1, 2]. It is common to normalize survey speed to a unit bandwidth or relative to another instrument for comparison. This is referred to as survey efficiency.

Selecting the best antenna geometry as to maximize the instrument survey speed requires many design trade-offs to be negotiated: size, cost, electronic placement, processing data rates, noise performance, signal strength, frequency response, and sensitivity ripple across neighboring beam patterns. The survey efficiency metric is a succinct way to capture the quality of a candidate design and help direct changes for further optimizations. Survey efficiency is estimated by a numerical analysis model for each candidate design.

Modeling begins with a full wave computation of a single antenna producing the embedded element pattern. This element pattern is included as part of a larger geometry for full wave simulation of the entire array and subsequently to propagate the fields onto a physical optics model of the Arecibo Telescope. Mutual impedance parameters between ports and embedded far fields from each antenna are included. After radiating through each reflector, the simulated radiation patterns are used to compute the array response to a plane wave arriving from a point in the sky. The

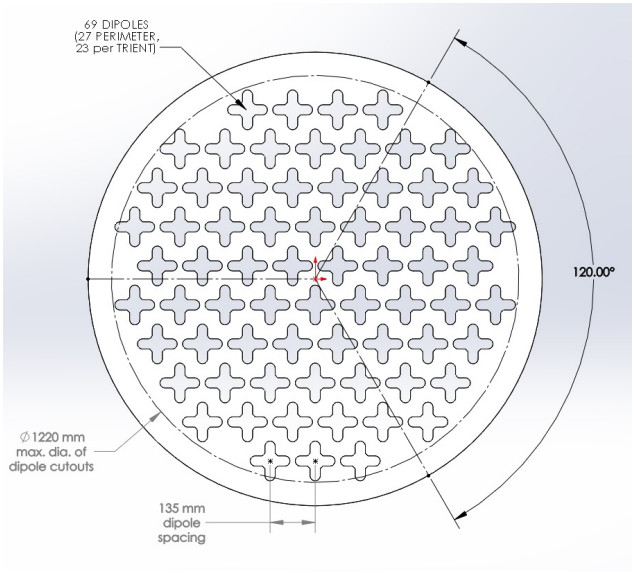

Figure 1. Hexagonal array layout with 69 dipole elements placed in three sections.

array response is used to form beams for each pixel, producing an estimate of the aperture efficiency across the FoV. The system noise temperature is estimated from measured noise parameters of the LNAs, calculated correlations derived from the impedance parameters of the antennas, and spatial models of spillover noise from the telescope geometry. Having computed aperture efficiency and system noise temperature over each steering angle in the FoV the survey efficiency metric can be calculated for a candidate element and array geometry design.

Several iterations of design optimization have taken place with the initial geometry modeling resulting in favor of a hexagonal array over a rectangular one [3]. Since then, continued optimizations of the hexagonal array have produced further tuning of the dipole, element orientation, and relative spacing to produce the final design as shown in Figure 1. The improvement in survey efficiency over the initial hexagonal array is shown in Figure 2. This new design greatly increases the survey efficiency over the bandwidth of the front end. More importantly, it achieves our design goal with peak performance near 1.4 GHz.

2.2 Dipole and LNA

The ALPACA front end is fully cryogenic. This differs from other L-band cryogenic PAFs in that thermal noise due to antenna losses is eliminated by placing the elements behind a thermal window and cooling them as a joint LNA/dipole module. The assembly is a cylindrical package and has press fit connectors at the base for easy servicing and replacement inside the cryostat.

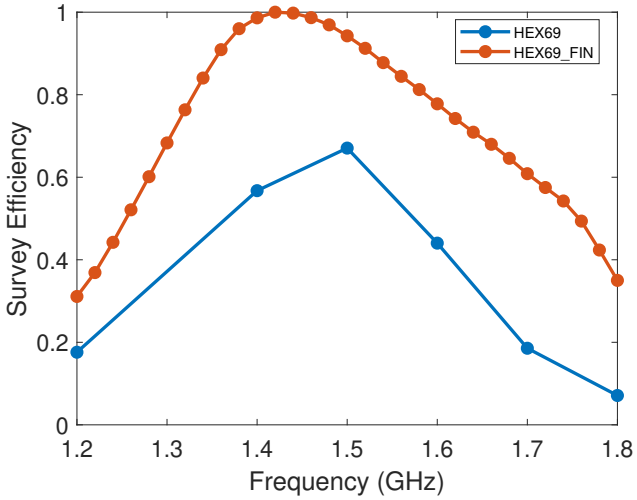

Figure 2. Improvement in survey efficiency over the previous candidate design following further design optimizations.

2.3 Dewar and Cryogenics

The cryostat has a radio-transparent high-density polyethylene (HDPE) vacuum window with a unique top-hat dome design. The dome structure is internally supported by three layers of Rohacell foam, which are also transparent at L-band. Three CTI 1020 cold heads provide the thermal load lift in two stages: an 80 K thermal sink for the ground plane followed by a 20 K thermal sink for the LNA/dipole package. The atmospheric load is transferred from the front window through the foam and 80 K first stage to the back of the cryostat supported by G10 tabs. This technique for supporting a very large window without any metallic dewar walls was successfully demonstrated with a 70 cm diameter window of identical design in [4].

The cryostat will be supported on the Gregorian dome rotary floor of the telescope receiver room. This will place the ground plane of the dipoles at the focal plane of the reflector optics. The instrument will include a mechanical rotator to track the changing parallactic angle during a typical observation.

3 Signal Transport – RFoF

The analog signal from each antenna must be transmitted a distance of approximately 610 m (2000 ft) from the hanging receiver dome to the control building instrument room for digital processing, while maintaining an overall system noise temperature at or below the design goal of 25 K. We have selected RFoF to accomplish this, as it avoids the high loss of coaxial cable and allows for a low noise link without repeaters. Our design uses a direct modulated laser diode, with a dedicated single-mode fiber for each antenna signal polarization. It is based on the RFoF link designed at McGill University for CHIME [5], modified for use at L-band.

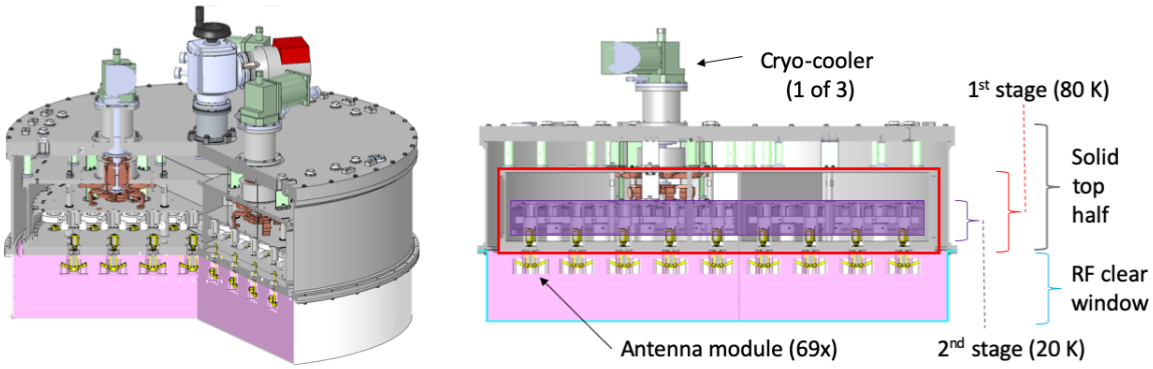

Figure 3. Cryostat design showing the LNA/dipole module within the radio-transparent HDPE vacuum window.

The RFI environment at Arecibo includes multiple high-powered radars, as well as weaker interference sources. The peak interference to noise ratio (INR) for ALPACA is expected to be at least 55 dB at the antennas, based on past measurements at the site. Dynamic range is a priority in the design of the signal transport system, to enable distortion-free observation in the presence of RFI. The RFoF link must have a dynamic range greater than the INR at its input, which is estimated to be at least 49 dB. The RFSoC ADC is 12-bit, providing additional dynamic range compared to the 8-bit ADC of CHIME. To utilize the full dynamic range of this ADC, the dynamic range of the RFoF must also increase. To this end, we have substituted a distributed feedback (DFB) laser diode with higher responsivity and lower noise than the original Fabry-Perot laser. Custom bandpass filters will precede the RFoF transmitter with a designed attenuation of 9 dB at the frequency of the strongest interferer at 1261 MHz.

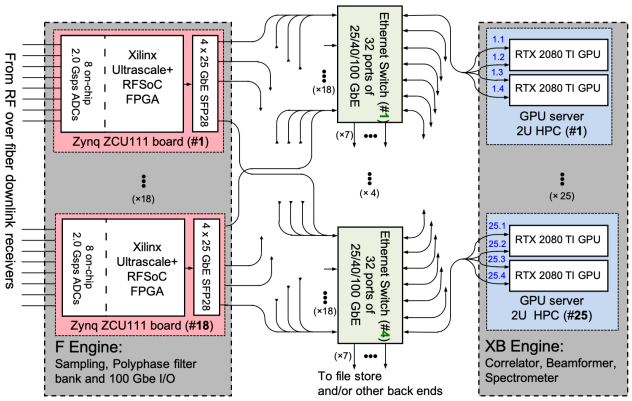

Figure 4. Signal processing is distributed over two stages. Antenna voltage signals are digitized and channelized in the first stage by 18 ZCU111 RFSoC boards. These data products are transported over 100 GbE for beamforming by a cluster of 25 HPCs each with two NVIDIA GPUs.

4 Digital Back End

The digital back end design is a heterogeneous architecture consisting of FPGAs and a cluster of GPU processing nodes networked with a 100 GbE spine. This architecture is shown in Figure 4 and has the advantage of creating an efficient multi-stage data processing pipeline.

First stage processing (F-engine) is implemented in the FPGAs and is responsible for digitizing the antenna voltages and producing the initial coarse bandwidth frequency channels. We will be using the Xilinx ZCU111 RFSoC to accomplish this. Among a few of its features, the RFSoC platform integrates several multi-gigasample per second ADCs with digital down conversion alongside the FPGA fabric. This allows for direct sampling at L-band, removing the need for other analog receiver components. Sampling all 138 antenna voltages will require 18 ZCU111 boards each processing eight, independently. Efficient frequency channelization is achieved using a 2048-point polyphase filter bank (PFB). However, this PFB is not the critically sampled PFB that is conventionally found in this architecture. Instead, we will implement an oversampled PFB as to enable the fine channel or zoom mode spectrometer in the second stage GPU nodes (XB-engine) without introducing spectral aliasing and amplitude scalloping in the spectra.

The XB-engine is implemented using 50 NVIDIA GPUs distributed over 25 high performance computers (HPCs). Among the digital back end operational modes will be array calibration for beamformer weight calculation, a coarse spectrometer with 244 kHz of separation between channels, and a fine spectrometer where an additional critically sampled PFB is implemented in the GPU producing narrower channels 5 kHz wide. In all science processing modes the real-time beamformer produces 40 simultaneous dual polarized beams steered within the FoV of the telescope. Array calibration mode uses the array covariance estimates formed on a regular grid of pointing towards a strong deep space calibration source. A calibration pointing is needed in each direction a beam is to be steered.

5 Conclusion

ALPACA is a new wide-field fully cryogenic PAF receiver for the Arecibo Telescope with the goal of operating at an effective system noise temperature of 25 K. The improved sensitivity and increased number of beams that more efficiently fill the FoV will greatly improve the survey speed at Arecibo. This enables the potential for pulsar and Fast Radio Burst searches, hydrogen surveys of the local universe, and many other important observations of the transient radio sky.

6 Acknowledgements

This material is based upon work supported by the National Science Foundation under Grant No. 1636645.

References

[1] K. F. Warnick, R. Maaskant, M. V. Ivashina, D. B. Davidson, and B. D. Jeffs, *Phased Arrays for Radio Astronomy, Remote Sensing, and Satellite Communications*. Cambridge University Press, 2018.

[2] J. Cordes, “Survey Metrics", *Square Kilometre Array Memo Series*, Oct. 2007.

[3] K. F. Warnick, J. Kunzler, and G. Cortes-Medellin, “Geometry Optimization of a Phased Array Feed on the Arecibo Telescope for Maximum Survey Efficiency” *IEEE International Symposium on Antennas and Propagation*, July 2019, pp. 399-400, doi:10.1109/APUSNCURSINRSM.2019.8888810.

[4] G. Cortes-Medellin, A. Vishwas, S. C. Parshley, D. B. Campbell, P. Perilatt, R. Black, J. Brady, K. F. Warnick, and B. D. Jeffs, “A Fully Cryogenic Phased Array Camera for Radio Astronomy” *IEEE Transactions on Antennas and Propagation*, vol. 63, no. 6, pp. 2471-2481, 2015.

[5] J. Mena, K. Bandura, J.-F. Cliche, M. Dobbs, A. Gilbert, and Q.Y. Tang, “A Radio-Frequency-over-Fiber link for large-array radio astronomy applications,” *Journal of Instrumentation*, **8**, 10, October 2013, doi:10.1088/1748-0221/8/10/T10003